Journal of Ultrafine Grained and Nanostructured Materials
https://jufgnsm.ut.ac.ir
Vol. 52, No.2, December 2019, pp. 149-153
Print ISSN: 2423-6845 Online ISSN: 2423-6837
DOI: 10.22059/jufgnsm.2019.02.03

Synthesis of Three - Dimensional Mesoporous Silicon from Rice Husk via SHS Route

Sepehr Mohajerani, Cyrus Zamani*, Abolghasem Ataie

School of Metallurgy and Materials Engineering, College of Engineering, University of Tehran, Tehran, Iran.

Recieved: 2 November 2019; Accepted: 29 November 2019
** Corresponding author email: c.zamani@ut.ac.ir*

ABSTRACT

Silicon nanoparticles are the focus of attention thanks to their potentialities in advanced applications such as new batteries, photovoltaic cells and so on. The need to porous silicon is thus rising and will follow the same trend. In this work, highly porous nanostructured silicon is synthesized via Self-propagating high-temperature synthesis (SHS) route. Microstructural and phase analyses show that the employed technique is capable of producing a three-dimensional porous silicon which can act as a skeleton for embedding lithium ions and therefore, resisting large volume expansions arising during lithiation phase. Considering the fact that the wave front experiences high temperatures (above 1900°C) which can result in nanoparticles' sintering, and in order to improve the porosity level, ammonium nitrate is used as a neutral additive at Mg/SiO_2/NH_4NO_3 (2.4:1:0.1) molar ratio. The influence of nitrate addition on the final microstructure is studied through comparing salt-added samples with bare ones. Results show that ammonium nitrate can hinder the agglomeration of silicon nanoparticles during the progress of combustion wave thus affecting the specific surface area significantly (138.3 $m^2 g^{-1}$ as compared to for the 43.8 $m^2 g^{-1}$ for the reference sample which lacks NH_4NO_3). On the other hand, it was found that the added salt does not affect the product purity as examined through X-ray diffraction analysis.

Keywords: *Mesoporous Silicon, SHS, Rice Husk, Silica Nanoparticles, Lithium-ion Battery*

1. Introduction

Rice Husk (RH) is considered as a waste material in rice fields but it has numerous advanced applications [1-5]. 15-20%wt of RH consist of silica which is in nanostructure form. This silica is a valuable material for many applications such as producing silica gels, pharmaceutical products, and ceramics. But the most interesting research has been done in reducing this Nano-silica to silicon because of the increasing demand to porous silicon as anode material for lithium-ion batteries (LIBs). Silicon shows a high theoretical capacity around ~4000 mAh/g as compared to conventional graphite anode (~370 mAh/g) used in LiBs. The other side of the coin is that this material comes with a major disadvantage being large volume expansion during lithiation/delithiation process which leads to pulverization of silicon anode and capacity fading. Porous silicon can be a solution to this problem according to the literature [6]. Pores in silicon structure can accommodate lithium-ions easily without considerable expansion thus leading to improved anode stability during cycling. Besides, porous silicon offers a high accessible surface area to the liquid electrolyte, which facilitates the fast ion transport. In the meantime, pore walls with

a thickness of less than 10nm in porous silicon facilitate diffusion of lithium ion by shortening diffusion paths and so the rate capabilities of electrodes improve [7,8].

Knowing all above, production of high purity silicon in an economical and green process still is a challenge. Silicon can be produced via Siemens process by hydrogenous reduction of trichlorosilane $SiHCl_3$. This process is intensive energy consuming and expensive so it can't be considered as a scalable and economical process [9]. Carbothermic process in another way to synthesis silicon usually on industrial scale but the main byproduct of this method is carbon dioxide that has undesired greenhouse effect. Silica can be reduced to silicon by conventional reactions such as calciothermic, aluminothermic, or magnesiothermic reactions of which, the latter is considered as the most promising process since it does not lead to formation of highly-stable non-removable byproducts [10]. Self-propagating high-temperature synthesis or combustion synthesis [11] is an attractive method for preparation of nanomaterials in which, a heterogeneous exothermic mixture of raw materials is consolidated to a disk shape sample and ignited at one end.

Short synthesis time, almost zero energy consumption (due to the exothermic nature of the reactions, and high purity products are among the advantages. Here we introduce a new way to synthesis porous silicon for Li-ion battery application by an economic, simple and scalable method.

2. Experimental

Details of silica preparation is reported elsewhere [12]. Briefly, Rice Husk washed with distilled water to remove the moisture for 1h followed by refluxing into dilute hydrochloric acid (1%w) in a 1000 ml flask at room temperature for an hour under stirring. The residue was filtered and washed with distilled water and dried at 100°C overnight prior to further processing. The leached material was calcined at 700 °C in air for 3h to achieve high purity silica powder. To obtain porous silicon, Silica powder was premixed with Mg powder (0.06-0.3 mm, Merck) in Mg/SiO_2 molar ratio of (1:2.4) (Si-r) and another sample with NH_4NO_3 in a $Mg:SiO_2:NH_4NO_3$ molar ratio of (1:2.4:0.1) (Si-n). When leached, samples are coded as Si-r-L and Si-n-L respectively.

SHS samples were prepared by cold pressing of the powder mixtures under a pressure of about 0.1 MPa. Disk-shape samples were placed in SHS chamber. To avoid oxidation of silicon during SHS, the chamber was filled by argon (Ar). The combustion setup works with 10A (current) and 6V (voltage). To remove the impurity phases, combustion products leached by an acidic solution with the following conditions: HCl (1.25M) 80%Wt: CH3COOH (4.38M) 20%Wt [9]. Leached products were washed with distilled and dried in 100°C for 1h. The crystal structure of samples was analyzed using X-ray powder diffraction (XRD) using Rigaku Ultima IV diffractometer at room temperature with Cu-Kα radiation (λ=1.5405 Å) in the range of $20°<2\theta<80°$ and with the step size of 0.02°. Scanning electron microscopy (SEM; CAMSCAN MV2300) was employed to investigate the products morphologically. The mean crystallite size of the powders was calculated by Scherrer equation (eq. 1):

$$D=(K.\lambda)/(\beta.\cos\theta) \quad \text{(eq. 1)}$$

where D is the crystallite size in nanometer, K is a shape factor (equal to 0.9), λ is the wavelength of Cu Kα radiation, θ is the Bragg angles of the major diffraction peaks, and β is the full width at half maximum (FWHM) of XRD peaks. The nitrogen adsorption and desorption isotherms were obtained using the Brunauer- Emmett-Teller (BET) method at 77 K after degassing the samples at 200 C for 1 h (BELSORP MINI II). The Barrett-Joyner-Halenda (BJH) method was applied to adsorption branches of isotherms to obtain pore radius distributions.

3. Results and Discussion

Rietveld analysis of the samples (using MAUD software) shows that about 82 wt% of rice husk is removed during purification process (i.e. calcination and leaching). The emergence of a large broad peak at about 22° in XRD pattern of the calcined samples (Fig. 1a) confirms the formation of amorphous silica from rice husk. SEM micrograph (Fig. 1b) shows a mean particle size of about 25 nm determined using Image J software. It noteworthy that achieving this microstructure (Fig. 1b) is possible only with the one-step leaching because HCl removes metallic impurities (Na, K, Ca, etc.) via formation of water-soluble metal chlorides and hindering formation of oxides such as Na6Si8O19 (such oxides melt at temperatures as low as about 740°C and cause sintering of silica nanoparticles).

XRD patterns of the Si-n samples after magnesiothermic reaction (conducted through SHS) reveals that in addition to silicon and MgO, in addition to MgO (which is formed according to reaction (1)), Mg_2SiO_4 is also produced as byproduct (Fig. 2a) while in the case of Si-r mixed with excess amount of magnesium(Fig. 2c), Mg_2Si is the byproduct formed through via reaction (2) [13, 14].

$SiO_2(s) + 2Mg(s) = Si(s) + 2MgO(s)$ (Reaction 1)
ΔH= -291.62 kJ mol^{-1}

$Si(s) + 2Mg(s) = Mg_2Si(s)$ (Reaction 2)
ΔH= -318.91 kJ mol^{-1}

Leaching of the combustion products leaves traces of Mg_2SiO_4 in Si-n-L samples as impurity (Fig. 2c) due to the fact that this phase is highly stable and its removal is complicated. However, in the case of Si-r-L material, no impurity is detected (Fig. 2d).

The temperature of combustion wave in this thermite reaction reaches 1900 °C (recorded using pyrometer) which is above the melting points of SiO_2 (1710 °C), Mg (650 °C) and Si (1414 °C). This temperature is also above the boiling point of Mg (1091 °C) but below the melting point of MgO (2852 °C). By adding NH4NO3 as a neutral additive to the mixture this temperature increase because of exothermic decomposition of NH4NO3 according to the reaction (3).

$NH_4NO_3(s) = N_2O(g) + 2H_2O(g)$ (Reaction 3)
ΔH= -36.54 kJ mol^{-1}

The reason behind formation of Mg2SiO4 in Si-n samples is that the high temperature of combustion wave leads to evaporation of more Mg so that a lack

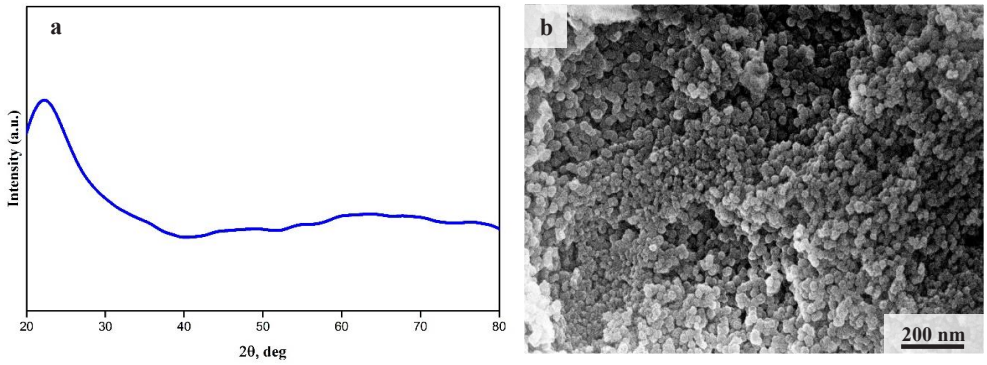

Fig. 1- Powder X-ray diffraction (XRD) pattern of obtained silica from rice husk (a) and Scanning electron microscopic (SEM) images of the obtained silica from rice husk (b).

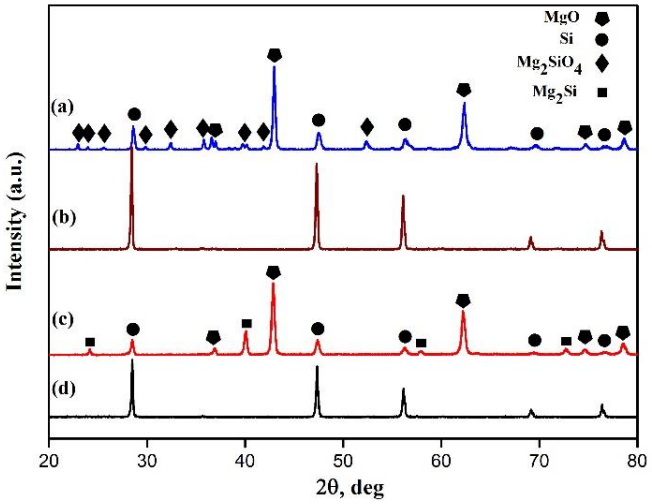

Fig. 2- Powder X-ray diffraction (XRD) pattern of (a) as-synthesized powder (Si-n), (b) porous silicon product (Si-n-L), (c) as-synthesized powder (Si-r) and (d) silicon product (Si-r-L).

of magnesi-um is sensed in the medium thus acting as a driving force for reaction (4).

$2MgO(s) + SiO_2(s) = Mg_2SiO_4(s)$ (Reaction 4)
ΔH= -56.61 kJ mol-1

Figure 3(a, b) shows SEM micrographs of leached samples, Si-r-L and Si-n-L respectively. A completely agglomerated microstructure is seen in Si-r-L sample possibly due to the fact that, reduced silicon is formed in a liquid state at the first stage and the available intense heat in the reaction medium forces silicon particles to agglomerate (Fig. 3a). However, Si-n-L with NH_4NO_3 as an effective additive shows a honeycomb structure with fully porous morphology (Fig. 3b). Energy-dispersive spectroscopy (EDS) analysis results in Fig. 3 shows silicon as the main element with a very slight amount of magnesium and oxygen impurity.

Adsorption isotherms and BJH curves in Fig. 4 help to better understand the microstructural evolution of the materials during synthesis. The Si-n-L porous structure is possibly formed by means of two different mechanisms according to the BJH curves illustrated in Fig. 4c,d. 1) Larger pores which are formed after washing MgO grains by acid leaching are observed in both BJH curves of both samples at around 10 nm r_p. 2) Pores with lesser diameter about 5nm r_p are seen only in Si-n-L BJH curve. These form when NH_4NO_3 decomposes and gas evolution occurs according to reaction (3). As a matter of fact, Si is melted in the wave front and gas bubbles are entrapped inside thus leaving small pores in the structure. The isotherms, in addition, are of type IV (IUAPAC standard) which is an indication of mesoporous structure. Brunauer-Emmett-Teller (BET) measurements show specific surface area (SSA) of 138.3 $m^2 g^{-1}$ and mean pore diameter of 18.5 nm for Si-n-L, while in the case of Si-r-L sample, these values were found to be 43.8 $m^2 g^{-1}$ and 24.6 nm respectively. Scherrer analyses based on the XRD pattern of leached products gives mean crystallite sizes of about 55 nm and 46 nm for Si-r-L and Si-n-L respectively. Such difference in crystallite size implies that NH_4NO_3 can also affect the nucleation of melted Si in the combustion wave.

4. Conclusions

Porous nanostructured silicon was obtained through a facile route.. Formation of a mesoporous structure was confirmed via both SEM as well as BET analyses. Ammonium nitrate showed a significant influence on the microstructure of final product as a neutral an additive changing SSA significantly in comparison to the reference

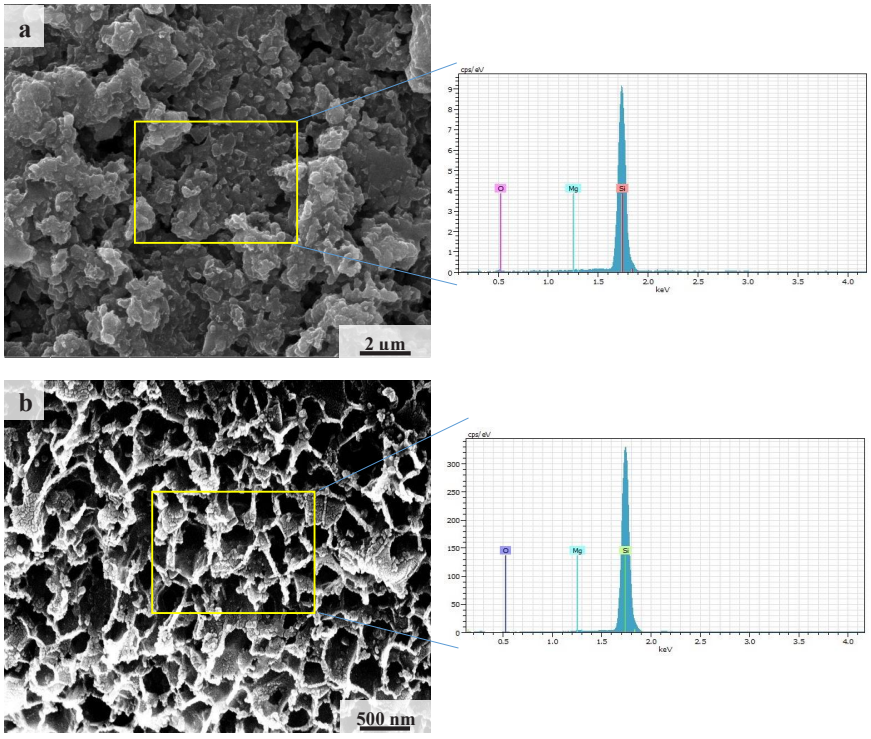

Fig. 3- SEM micrograph of porous silicon product (Si-r-L) (a), silicon product (Si-n-L) (b).

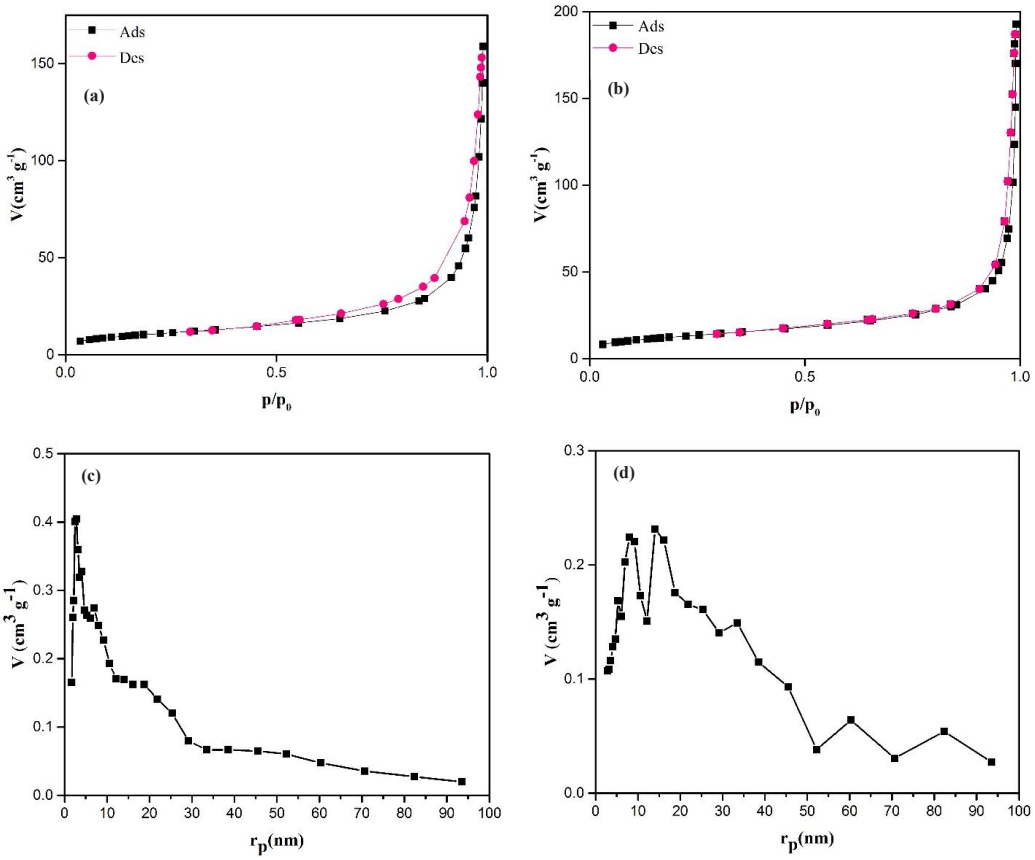

Fig. 4- N_2 adsorption-desorption isotherms of porous silicon product Si-n-L (a) , silicon product Si-r-L (b), BJH pore size distribution of Si-n-L (c) and Si-r-L (d).

sample. Complete removal of Mg2SiO4 from the products was found to be rather difficult due to the high stability of the silic phase.

References

1. Alvarez J, Lopez G, Amutio M, Bilbao J, Olazar M. Upgrading the rice husk char obtained by flash pyrolysis for the production of amorphous silica and high quality activated carbon. Bioresource Technology. 2014;170:132-7.
2. Soltani N, Bahrami A, Pech-Canul MI, González LA. Review on the physicochemical treatments of rice husk for production of advanced materials. Chemical Engineering Journal. 2015;264:899-935.
3. Sun L, Gong K. Silicon-Based Materials from Rice Husks and Their Applications. Industrial & Engineering Chemistry Research. 2001;40(25):5861-77.
4. Wang W, Martin JC, Fan X, Han A, Luo Z, Sun L. Silica Nanoparticles and Frameworks from Rice Husk Biomass. ACS Applied Materials & Interfaces. 2012;4(2):977-81.
5. Jung DS, Ryou MH, Sung YJ, Park SB, Choi JW. Recycling rice husks for high-capacity lithium battery anodes. Proceedings of the National Academy of Sciences. 2013;110(30):12229-34.
6. An W, Gao B, Mei S, Xiang B, Fu J, Wang L, et al. Scalable synthesis of ant-nest-like bulk porous silicon for high-performance lithium-ion battery anodes. Nature Communications. 2019;10(1).
7. Zhao S, Xu Y, Xian X, Liu N, Li W. Fabrication of Porous Si@C Composites with Core-Shell Structure and Their Electrochemical Performance for Li-ion Batteries. Batteries. 2019;5(1):27.
8. Gao P, Tang H, Xing A, Bao Z. Porous silicon from the magnesiothermic reaction as a high-performance anode material for lithium ion battery applications. Electrochimica Acta. 2017;228:545-52.
9. Xakalashe BS, Tangstad M. Silicon processing: from quartz to crystalline silicon solar cells.
Sothern African Pyrometallurgy. 2011; 83-100.
10. Larbi KK, Barati M, McLean A. Reduction behaviour of rice husk ash for preparation of high purity silicon. Canadian Metallurgical Quarterly. 2011;50(4):341-9.
11. Liu PS, Chen GF. Applications of Porous Ceramics. Porous Materials: Processing and Applications, Elsevier Science & Technology, 1st edition. 2014.
12. Azadeh M, Zamani C, Ataie A, Morante JR. Three-dimensional rice husk-originated mesoporous silicon and its electrical properties. Materials Today Communications. 2018;14:141-50.
13. Liu N, Huo K, McDowell MT, Zhao J, Cui Y. Rice husks as a sustainable source of nanostructured silicon for high performance Li-ion battery anodes. Scientific Reports. 2013;3(1).
14. Bao Z, Weatherspoon MR, Shian S, Cai Y, Graham PD, Allan SM, et al. Chemical reduction of three-dimensional silica micro-assemblies into microporous silicon replicas. Nature. 2007;446(7132):172-5.